Journal of materials and Environmental Sciences
ISSN : 2028-2508

Copyright © 2017,
University of Mohammed Premier
Oujda Morocco

JMES, 2017 Volume 8, Issue 1, Page 225-237

http://www.jmaterenvironsci.com/

Corrosion inhibition of mild steel by two new 1,2,4-triazolo[1,5-a] pyrimidine derivatives in 1 M HCl: Experimental and computational study

S. Lahmidi[1], A. Elyoussfi[2], A. Dafali[2], H. Elmsellem[2*], N. K. Sebbar[1], L. El Ouasif[1], A. E. Jilalat[1], B. El Mahi[2], E. M. Essassi[1,3], I. Abdel-Rahman[4] and B. Hammouti[2]

[1]*Laboratoire de Chimie Organique Hétérocyclique, URAC 21, Pôle de Compétences Pharmacochimie, Mohammed V University Rabat, Faculté des Sciences, Av. Ibn Battouta, BP 1014 Rabat, Morocco.*
[2] *Laboratoire de chimie analytique appliquée, matériaux et environnement (LC2AME), Faculté des Sciences, B.P. 717, 60000 Oujda, Morocco.*
[3]*Moroccan Foundation for Advanced Science, Innovation and Research (MASCIR), Rabat Design Center, Rue Mohamed Al Jazouli, Madinat El Irfane, Rabat, Morocco.*
[4]*Department of Chemistry, College of Sciences, University of Sharjah, PO Box: 27272, UAE.*

Received 22 Oct 2016,
Revised 28 Nov 2016,
Accepted 04 Dec 2016

Keywords
- ✓ 1,2,4-triazolo[1,5-a]pyrimidine,
- ✓ EIS,
- ✓ Corrosion,
- ✓ Mass loss,
- ✓ Electrochemical,
- ✓ DFT,
- ✓ Fukui function.

h.elmsellem@yahoo.fr / +212670923431

Abstract

The inhibition ability of two new 1,2,4-triazolo[1,5-a]pyrimidine derivatives (P3 and P4) towards mild steel corrosion in 1 M HCl solution was studied at various concentrations and temperatures using mass loss, polarization curves, and electrochemical impedance spectroscopy (EIS)methods. The experimental results reveal that P3 and P4 are efficient mixed type corrosion inhibitorsand their inhibition efficiencies increase with increasing concentration. The adsorption of these inhibitors on mild steel surface obeys Langmuir isotherm. Quantum chemical parameters were calculated using the Density Functional Theory method (DFT). The Correlation between theoretical and experimental results was discussed.

1. Introduction

The study of the corrosion inhibition of metallic surfaces (MS) against the corrosion in acid solutions by inhibitors is an important industrial topic and highly powerful subject of research. Acidic environments, especially hydrochloric acid solutions (HCl), are widely used in various industrial processes, such as oil well acidification, acid pickling, acid cleaning, and acid descaling, which generally leads to serious metallic corrosion [1–3]. Organic compounds are good inhibitors of the electrochemical corrosion of metals [4]. The most effective and efficient organic compounds have heteroatoms, such as phosphorus, sulfur, nitrogen, and oxygen (P, S, N, and O, respectively), and compounds with aromatic rings in their structures [5–11], which are important characteristic features that determine the adsorption centers of inhibitor on the metal surface and separate the effective inhibitors from the others. Although these compounds exhibit good inhibition properties, their use has caused several negative effects on the environment because of their toxicity and non-biodegradability [12, 13].

In this regard, Pyrimidine derivatives continue to attract great interest due to the wide variety of interesting biological activities observed for these compounds, such as anticancer [14], antiviral [15], antitumor [16], anti-inflammatory [17], antimicrobial [18], antifungal [19], antihistaminic [20] and analgesic [21] activities. Consequently, The condensation of a ring of 1,2,4-triazole and another one of pyrimidine gives rise to the formation of bicyclic heterocycles known as 1,2,4-triazolopyrimidines.

1,2,4-Triazolo [1,5-a] pyrimidine derivatives are thermo-dynamically more stable and , thus, the most studied ones [22]. Recently, research became intensified on the synthesis of these compounds [23-27]. The study of these compounds has been aroused increasing attention from the chemical and biological view points, due to their diverse pharmacological activities, such as antitumor potency[28-31], antimalarial [32], antimicrobial[33-36], anti-inflammatory [37], inhibition of KDR kinase [25], antifungal [38] and macrophage activation [39].

The reaction of 3-amino-1,2,4-triazole or 3,5-diamino-1,2,4-triazole with 4-hydroxy-6-methyl-pyran-2-one to form 1,2,4-triazolo[1,5-*a*]pyrimidine derivatives P3 and P4 was recently published [40, 42]. The chemical structure of P3 and P4 was shown in (Figure 1).

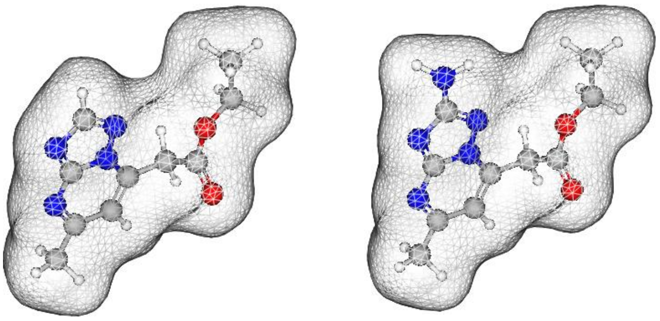

P3 P4

Figure 1. Chemical structure of 1,2,4-triazolo[1,5-a]pyrimidine derivatives (**P3** and **P4**).

2. Experimental

2.1. Specimens and Solutions Preparation

Mass loss tests were carried out on mild steel specimen of chemical composition: C-0.05 %, Mn-0.6%, P-0.36%, Si-0.03% and the remainder iron. Mild steel specimens were used in the sheet form of 1.5 cm × 1.5 cm × 0.5 cm dimensions**.** Before mass loss test, mild steel specimens were cleaned with acetone, dried and stored moisture free desiccators. The aggressive solutions of 1.0 M HCl were prepared by dilution of analytical grade 37% HCl with distilled water. The concentration range of P3 and P4 employed was 10^{-6}M – 10^{-3}M in 1M HCl solutions.

2.2. Synthesis of inhibitor

A mixture of the 3-amino-1, 2, 4-triazole (P1) or 3,5-diamino-1,2,4-triazole (P2) (10 mmol) and 4-hydroxy-6-methyl-2H-pyran-2-one (12.5 mmol) in 30 ml of ethanol was refluxed for 12 hours. After cooling, the reaction mixture was allowed to stand overnight and then filtered to give the solid triazolopyrimidine products, which were crystallized from ethanol, (Scheme 1).

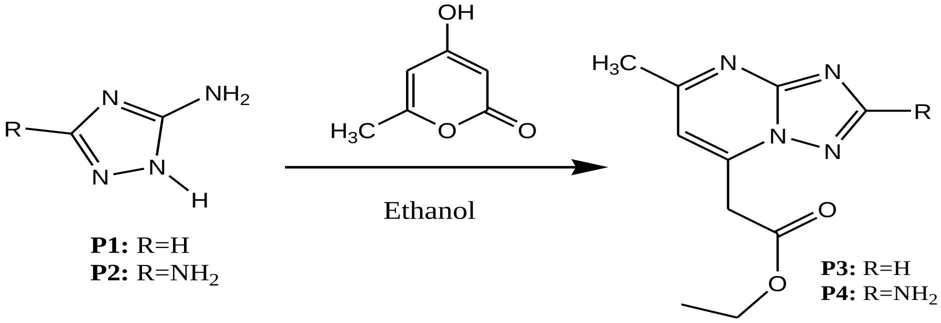

Scheme 1. Synthesis of 1,2,4-triazolo[1,5-a]pyrimidine derivatives (P3 and P4).

The analytical and spectroscopic data are conforming to the structure of compound formed:
(P3): Yield: 67%; **M.p: 511K**; **NMR^{1}H (DMSO-d6) δ ppm:** 2.46 (s, 3H, $-CH_3$); 1.02 (t, 3H, $-CH_3$); 4.40(s, 2H, CH_2); 3.98(q, 2H, CH_2); 6.86(s, 1H, H_{ar}); 8.15 (s, 1H, $H_{triazol}$); **NMR^{13}C (DMSO-d6) δ ppm:**13.63 ($CH_3$9); 24.68 (CH_3);35.71 (CH_2); 61.50 (CH_2); 111.38(CH_{ar}); 142.12($CH_{triazol}$) ; 154.74 (Cq), 154.84 (Cq); 164.71(Cq); 166.60(C=O).

(P4): Yield: 70%; **M.p: 437K**; **NMR^{1}H (DMSO-d6) δ ppm:** 2.46 (s, 3H, -CH_3);1.14 (t, 3H, -CH_3); 3.81 (s, 2H, CH_2); 4.08(q, 2H, CH_2); 6.88 (s, 1H, H_{ar}); 4.07 (s, 2H, NH_2); **NMR^{13}C (DMSO-d6) δ ppm:** 24.57 (CH_3); 14.41 (CH_3); 61.49 (CH_2); 36.37 (CH_2); 109.61(CH_{ar}) ; 155.22 (Cq), 157.43 (Cq); 167.27(Cq); 161.89 (Cq); 167.90 (C=O).

2.3. Mass Loss Method

Mass loss is one of the easiest and widely used techniques of preliminary inhibition assessment. The pre-weighed and polished mild steel sheet was immersed in 100 ml of 1M HCl solution without and with various concentrations of P3 and P4 for 6 hrs at 308K.

After 6 hrs., the sheet was taken from the solution, washed with double distilled water, rinsed with acetone, dried and reweighed. The mass of each steel sheet was measured before and after immersion using an analytical balance. Tests were done in triplicate at the same time, and the average mass loss was calculated.

2.4. Electrochemical measurements

Electrochemical measurements, including stationary methods and transient (EIS) were performed in a three-electrode cell. Pure mild steel specimen was used as the working electrode, a saturated calomel (SCE) as reference electrode and an area platinum as counter electrode (CE) were used. All potentials were measured against CE. The working electrode was immersed in a test solution for 30 mins until the corrosion potential of the equilibrium state (E_{corr}) was achieved using a type PGZ100 potentiostat. The potentiodynamic polarization curves were determined by a constant sweep rate of 1 mv/s. The measurements of the transitory method (EIS) were determined; using ac signals of amplitude 10 mV peak to peak at different conditions in the frequency range of 100 kHz to 10 mHz.

2.5. Quantum chemical calculations

Quantum chemical calculations are used to correlate experimental data for inhibitors obtained from different techniques (viz., electrochemical and weight loss) and their structural and electronic properties. According to Koop man's theorem [43], E_{HOMO} and E_{LUMO} of the inhibitor molecule are related to the ionization potential (I) and the electron affinity (A), respectively. The ionization potential and the electron affinity are defined as $I = -E_{HOMO}$ and $A = -E_{LUMO}$, respectively. Then absolute electronegativity (χ) and global hardness (η) of the inhibitor molecule are approximated as follows [44]:

$$\chi = \frac{I+A}{2} \;,\;\; \chi = -\frac{1}{2}(E_{HOMO} + E_{LUMO}) \quad \textbf{(1)}$$

$$\eta = \frac{I-A}{2} \;,\;\; \eta = -\frac{1}{2}(E_{HOMO} - E_{LUMO}) \quad \textbf{(2)}$$

The fraction of transferred electrons ΔN was calculated according to Pearson theory [45]. This parameter evaluates the electronic flow in a reaction of two systems with different electronegativities, in particular case; a metallic surface (Fe) and an inhibitor molecule. ΔN is given as follows:

$$\Delta N = \frac{\chi_{Fe} - \chi_{inh}}{2(\eta_{Fe} + \eta_{inh})} \textbf{(3)}$$

Where χ_{Fe} and χ_{inh} denote the absolute electronegativity of an iron atom (Fe) and the inhibitor molecule, respectively; η_{Fe} and η_{inh} denote the absolute hardness of Fe atom and the inhibitor molecule, respectively. In order to apply the eq3 in the present study, a theoretical value for the electronegativity of bulk iron was used $\chi_{Fe} = 7$ eV and a global hardness of $\eta_{Fe} = 0$, by assuming that for a metallic bulk I = A because they are softer than the neutral metallic atoms [46,47].

The electrophilicity has been introduced by Sastri et al. [44], is a descriptor of reactivity that allows a quantitative classification of the global electrophilic nature of a compound within a relative scale. They have proposed the ω as a measure of energy lowering owing to maximal electron flow between donor and acceptor and ω is defined as follows.

$$\omega = \frac{\chi^2}{2\eta} \quad \textbf{(4)}$$

The Softness σ is defined as the inverse of the η [47]

$$\sigma = \frac{1}{\eta} \quad \textbf{(5)}$$

3. Results and discussion

3.1. Mass Loss Measurements

In the gravimetric experiment, a previously weighed metal (mild steel) coupon was completely immersed in 100 ml 1 M HCl solutionwithout and with different concentrations of P3 and P4 in an open beaker. The beaker was inserted into a water bath maintained at 308 K. From the mass loss results, the inhibition efficiency (E%) of the inhibitor and degree of surface coverage (θ) were calculated using equations 6 and 7[48]:

$$E\% = (1 - w_0 / w_i) * 100 \quad \textbf{(6)}$$

$$\theta = E\%/100 \quad \textbf{(7)}$$

Where w_0 and w_i are the mass losses formild steel in the absence and presence of the inhibitor in1 M HCl solution and θis the degree of surface coverage of the inhibitor.

The values of percentage inhibition efficiency and corrosion rate obtained from weight loss method at different concentrations at 308K are summarized in Table 1. Examination of values indicates clearly a net decrease in the corrosion rate of mild steel in the presence of the studiedinhibitors. In other words, their inhibition efficiency increased to reach a maximum value of 88% for P3 and 96% for P4 at 10^{-3}M.

This may be interpreted by the presence of this kind of cyclic rings and the heteroatoms facilitate the adsorption process. The variation in the degree of surface coverage and corrosion rate in the presence of these two compounds may be attributedto the addition of another N atom in P4: the efficiency increasedfrom 88% for P3 to 96 % for P4 at 10^{-3}M.

Table 1. Gravimetric results of mild steel in 1M HCl without and with different concentrations of each inhibitor at 308K for 6 hrs.

Inhibitor	Concentration of Inhibitor (M)	W_{corr} (mg.cm^{-2}.h^{-1})	E_w(%)	Surface Coverage (θ)
1 M HCl (without inhibitor)	-	0.91	--	-
P3 (in 1 M HCl)	**10^{-3}**	0.11	**88**	**0.88**
	10^{-4}	0.14	85	0.85
	10^{-5}	0.18	80	0.80
	10^{-6}	0.22	76	0.76
P4 (in 1 M HCl)	**10^{-3}**	0.04	**96**	**0.96**
	10^{-4}	0.07	92	0.92
	10^{-5}	0.15	89	0.89
	10^{-6}	0.14	85	0.85

3.2. Thermodynamic parameters of the adsorption process

3.2. 1. Adsorption isotherm

The organic corrosion inhibitor reacts in acidic media by adsorptionatthe metal/solution interface. The adsorption depends essentially on the structures and electronic properties of inhibitor compounds, such us, aromaticity, electronic density on donor atom ad the π orbital character of donating electrons [49, 50]. Furthermore, the solvent H_2O molecules can be adsorbed at the metal/solution interface. Therefore, the adsorption of organic inhibitor compounds from the aqueous solution can be considered as a quasi-substitution process between the organic molecules in the aqueous phase $Org_{(sol)}$ and water molecules at the electrode surface $H_2O_{(ads)}$ [51]:

$$Org_{(sol)} + xH_2O_{(ads)} \leftrightarrow xH_2O_{(sol)} + Org_{(ads)}$$

Where x is the size ratio, that is, the number of water molecules changed by one organic inhibitor. The adsorption isotherm can be giving information about the properties of the tested inhibitors. The degree of surface coverage (θ)values of the studied inhibitorsare calculated in order to determine the adsorption isotherm. In this study, degree of surface coverage (θ) valuesfor the concentrations of inhibitors range between 10^{-3}M and 10^{-6}M in 1 M HCl solutionshave been determined forthe P3 and P4 inhibitors and tabulated in Table 1.

For defined the mode of adsorption isotherm, different fit of the θ values to various isotherms, as well as, Temkin, Langmuir, Frumkin and Flory-Huggins, were made. The excellent fit is obtained with the Langmuir isotherm. Langmuir adsorption isotherm is described by the following equations:

$$\frac{\theta}{1-\theta} = K_{ads} C_{inh} \quad \textbf{(8)}$$

By rearranging this equation:

$$\frac{C_{inh}}{\theta} = \frac{1}{K_{ads}} + C_{inh} \quad \textbf{(9)}$$

Where K_{ads} is the adsorption equilibrium constant,C_{inh} is the inhibitor concentration, and θ is the surface coverage. Figure2 shows the plots of C_{inh}/θ versus C_{inh} and the estimated linear correlation is obtained for P3 and P4.

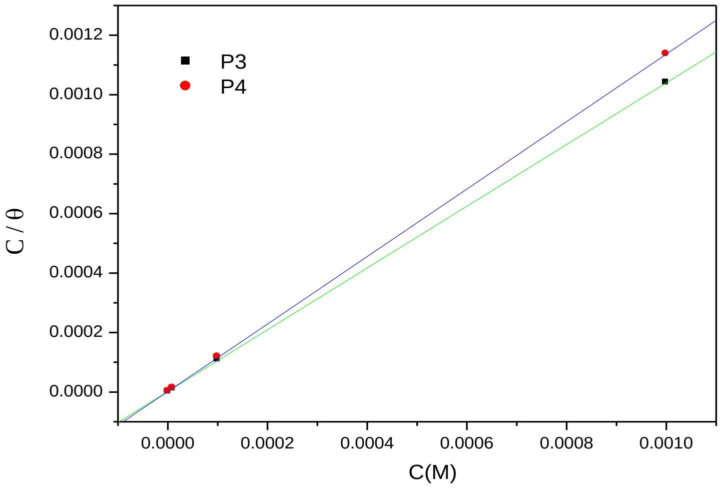

Figure 2. Langmuir adsorption isotherm plot for mild steel in 1M HCl at different concentrations of P3 and P4

The strong correlations(R^2=0.99999 and R^2=0.99998) confirm the validity of this approach. The adsorption equilibrium constant (K_{ads}) has been found to be 5.58E5 $M^{-1}$for P3 and 5.71E5 M^{-1} for P4(Table 2) suggesting that the adsorbed inhibitor molecules form monolayer on the mild steel surface and there is no interaction among the adsorbed inhibitor molecules [52]. On the other hand, the high value of adsorption equilibrium constant reflects the high adsorption capacity of P3 and P4 on mild steel surface [53, 54]. The standard free energy of adsorption (ΔG°_{ads}) can be determined by the following equation (10):

$$\Delta G^{\circ}_{ads} = -RT\ln(55.5K_{ads}) \quad \textbf{(10)}$$

Where R is the gas constant (8.314 J K^{-1} mol^{-1}), T is the absolute temperature (K), the value 55.5 is the concentration of water in solution expressed in M[55], and K_{ads} = 55.5 K_{eq}.

Table 2. Thermodynamic parameters for the adsorption of P3 and P4 in 1 M HCl on the mild steel at 308 K

Inhibitor	Slope	K_{ads} (M^{-1})	$-\Delta G^{\circ}_{ads}$ ($KJ.mol^{-1}$)	R^2
P3	1.04	5.58E5	44.15	0.99998
P4	1.13	5.71E5	43.20	0.99999

The ΔG°_{ads}value is calculated as-44.15kJ mol^{-1} for P3 and -43.20kJ mol^{-1} for P4. In the literature, if the absolute values of $\Delta G^{\circ}_{ads}$are less than20 kJ mol^{-1} consistent with the electrostatic interaction between the charged metal and charged molecules (physisorption), but if those more than 40 kJ mol^{-1} involve sharing or transfer of electrons from the inhibitor compound to the metal surface to form a co-ordinate type of bond (chemisorption) [56,57]. The values of ΔG°_{ads}calculated in this study are between 44.15 kJ mol^{-1}and 43.20 kJ mol^{-1}suggest that the adsorption of our inhibitors has the type of interactions: chemisorptions [58].

3.3. Corrosion inhibition studies

3.3.1. Polarization measurements

The electrochemical inhibition properties of P3 and P4 were analyzed by the polarization Tafel extrapolation. The polarization experiments were carried at different concentrations of inhibitors in order to estimate the corrosion rate at the electrode surface. The Tafel extrapolation was applied to determine the rate of corrosion or corrosion inhibition.

The inhibition efficiency was then calculated using the expression:

$$E_P\ \% = \frac{I^{\circ}_{corr} - I_{corr}}{I^{\circ}_{corr}} X\, 100 \qquad (\mathbf{11})$$

Where $I^{\circ}_{corr}$and $I_{corr}$are uninhibited and inhibited corrosion current densities, respectively.

The corrosion rates (Table 3) were measured after the metal surface exposure to corrosive medium for 0.5 h in the presence of compounds at different concentrations, manifesting that with the increasing inhibitor concentration, the corrosion rate continuously decreases; particularly, the corrosion potential does not suffer significantly. It indicates that the mechanism of corrosion inhibition of the metal surface is merely presenting an adsorption phenomenon that hampers both anodic and cathodic reactions.

The data show that in the presence of the inhibitor, the polarization current is considerably decreased, meaning that the intensity of corrosion is decreased. For instance, for the curve before the addition of P3 or P4 to the corrosive medium (1M HCl), the current density was 1386 µA/cm^2, and it was considerably reduced to 62 µA/cm^2 for P4 (10^{-3}M), and for P3, it was reduced to 72 µA/cm^2, observing that the current density is decreased in both cathodic and anodic branches (Figures 3 and 4).

Table 3. kinetic parameters calculated from Tafel extrapolation measurements after 30minsof immersion in 1M HCl solution without and with different concentrations of inhibtors at 308K.

Inhibitor	**Inhibitor (M)**	**E_{corr} (mV/SCE)**	**I_{corr} (µA/cm^2)**	**β_c (mV dec^{-1})**	**β_a (mV dec^{-1})**	**E_p (%)**
1 M HCl	-	-464	1386	-193	113	--
P4 (in I M HCl)	**10^{-3}**	-469	62	-100	73.9	**95**
	10^{-4}	-461	98	-105	75	92
	10^{-5}	-461	160	-109	76	88
	10^{-6}	-465	228	-192	89	83
P3 (in I M HCl)	**10^{-3}**	-452	172	-109	73.9	**87**
	10^{-4}	-454	213	-104	76	84
	10^{-5}	-457	313	-98	79.5	77
	10^{-6}	-453	348	-201	81	74

3.4. EIS studies.

The corrosion behavior of mild steel in 1 M HCl at temperature 308 K in the absence and presence of different inhibitors (P3 and P4) was investigated using electrochemical impedance spectroscopy. The Nyquist plots of mild steel in uninhibited and inhibited acid solutions (1 M HCl) are given in Figures 5 and 6. The electrochemical parameters calculated from the Nyquist plots are given in Tables 4.

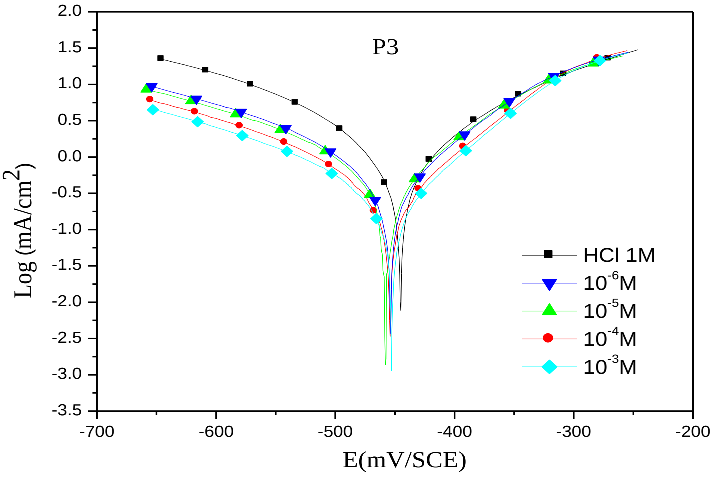

Figure 3. Potentiodynamic polarization curves for mild steel at 308 K in 1M HCl solution in the absence and the presence of various concentrations 0f P3.

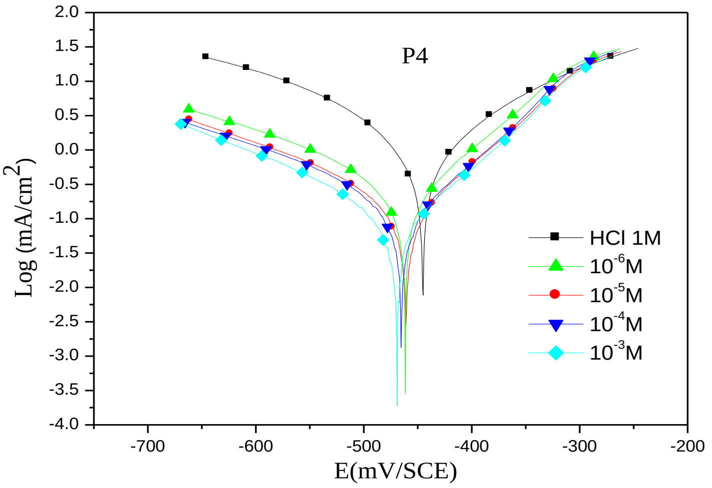

Figure 4. Potentiodynamic polarization curves for mild steel at 308 K in 1M HCl solution in the absence and the presence of various concentrations of P4.

The values of E% were calculated by using the following equation:

$$E\ \% = [1 - R_{ct}/R_{inh}] \qquad \textbf{(12)}$$

Here, R_{ct} and R_{inh} are charge-transfer resistance values in the absence and presence of the inhibitor, respectively. The Nyquist plots contain depressed semicircles with their center located under the real axis, and their size increases with the addition of inhibitors, indicating a charge transfer process mainly controlling the corrosion of mild steel [59,60]. Such a behavior is typical of solid electrodes and often referred to frequency dispersion, attributed to the surface heterogeneity due to surface roughness, impurities or dislocations [61], fractal structures, distribution of activity center, adsorption of inhibitors and formation of porous layers [62–65].The obtained impedance data were fitted to the electrical equivalent circuit (Figure 7) in order to model the mild steel/solution interface in the absence and presence of the inhibitor [66]. The circuit consists of Rs the electrolyte resistance, Rct the charge transfer resistance, and CPE the constant phase element. We have used CPE in the place of double layer capacitance (C_{dl}) in order to give a more accurate fit to the experimental results [67]. The use of CPE is required for modeling the frequency dispersion generally related to the surface heterogeneity [68].The form of the capacitive loops shows that the corrosion process was controlled by charge transfer. We noted that the obtained impedance responses were significantly changed by addition of different concentration of inhibitors. The diameter of these capacitive loops increases gradually with rise of inhibitors concentration of P3 and P4, indicating strengthening of inhibitive film.

The results of Table 4 show that the charge transfer resistance (R_{ct}) and efficiency (E%) increase with augmentation of inhibitors concentration. However, the value of double layer capacitance (C_{dl}) decreasesbecause it is inversely proportional with the charge transfer resistance atall concentrations. This result may be attributed to the formation of a protective layer on the electrode surface [69]. Impedance data from Table 4 show at 10^{-3}M P3 and 10^{-3}M P4 had maximum corrosion inhibitive effect for mild steel in 1M HCl at the studied temperature 308 K.

Table 4. Electrochemical impedance measurements for mild steel immersed in 1M HCl for 30minsin the absence and presence of different concentrations of inhibitors.

Inhibitor	**Inhibitor (M)**	**Rct (Ω.cm^2)**	**Cdl (μf/cm^2)**	**E (%)**
1M HCl	-	15	200	--
P3 (in 1M HCl)	**10^{-3}**	91	70	**84**
	10^{-4}	86	74	82
	10^{-5}	66	75	78
	10^{-6}	48	82	69
P4 (in 1 M HCl)	**10^{-3}**	200	50	**93**
	10^{-4}	168	59	91
	10^{-5}	104	61	85
	10^{-6}	75	86	78

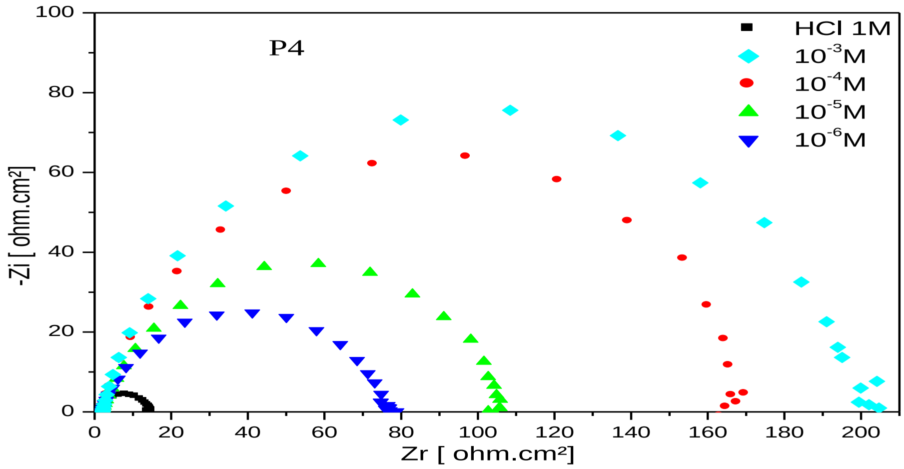

Figure 5. Nyquist plots for mild steel in 1 M HCl without and with various concentrations of the studied inhibitor P4 at 308 K.

The results show that the P3 and P4 inhibit the corrosion of mild steel in 1 M HCl solution at different concentration studied and the efficiency increase with rise of concentration at 308 K (table 4). The E(%) obtained from EIS techniques, mass loss and those calculated from polarization curves measurements are in good agreements for both inhibitors.

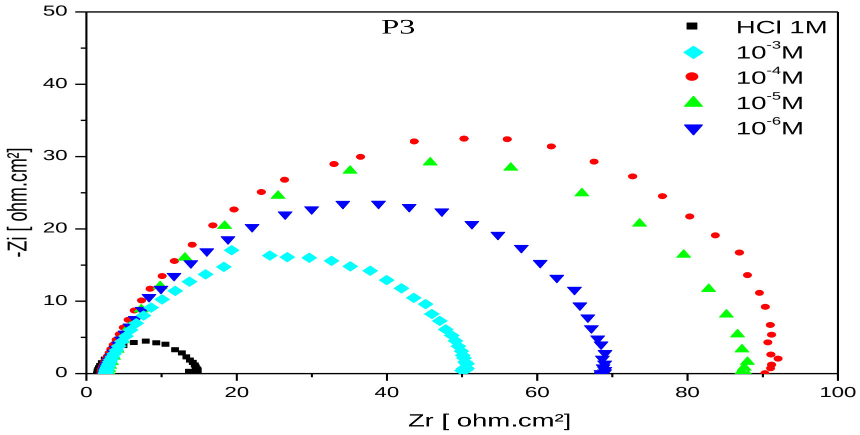

Figure 6. Nyquist plots for mild steel in 1 M HCl without and with various concentrations of the studied inhibitor P3 at 308 K.

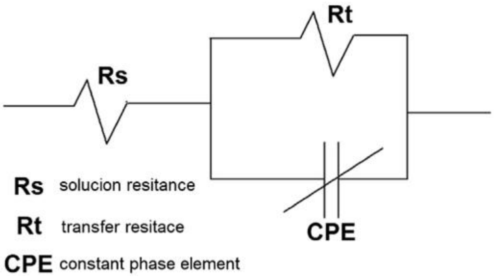

Figure7. Circuit electrical equivalent with one CPE.

3.5. Computational theoretical studies

In the last few years, the FMOs (HOMO and LUMO) are widely used for describing chemical reactivity. The HOMO containing electrons, represents the ability (E_{HOMO}) to donate an electron, whereas, LUMO haven't electrons, as an electron acceptor represents the ability (E_{LUMO}) to obtain an electron. The energy gap between HOMO and LUMO determines the kinetic stability, chemical reactivity, optical polarizability and chemical hardness–softness of a compound [70].

In this paper, the HOMO and LUMO orbital energies were calculatedby using B3LYP method with 6-31G. All other calculations were performed using the results with some assumptions. The higher values of E_{HOMO} indicate an increase for the electron donor and this means a better inhibitory activity with increasing adsorption of the inhibitor on a metal surface, whereas E_{LUMO} indicates the ability to accept electron of the molecule. The adsorption ability of the inhibitor to the metal surface increases with increasing of E_{HOMO} and decreasing of E_{LUMO}.

High ionization energy (I= 7.06 eV, I= 7.46 eV in gaseous and aqueous phases, respectively) indicates high stability [71-73]. The number of electrons transferred (ΔN) was calculated and tabulated in Table 5. The $\Delta N(gas) < 3.6$ and $\Delta N(aqueous) < 3.6$ indicates the tendency of a molecule to donate electrons to the metal surface [74].

The geometry of **P3** and **P4** in gaseous and aqueous phases (**Figure 8**) was fully optimized using DFT based on Beck's three parameters exchange functional and Lee–Yang–Parr nonlocal correlation functional (B3LYP)[75-76] and the 6–31G. The optimized molecular and selected angles, dihedral angles and bond lengths of **P3** and **P4** are given in (**Figure 8**). The optimized structure shows that the molecules P3 and P4 have a non-planar structure. The HOMO and LUMO electrons density distributions of **P3** and **P4** are given in (**Table 6**).

The large efficiency inhibition of P4 with respect to P3 is due to the presence of the amine group (NH_2) in P4 inhibitor, which contains an N atom with lone pair of electrons, which increases the electron donor character of P4 compared with P3. The theoretical data obtained are in good agreement with the experimental inhibition efficiency results earlier reported.

Table 5. Quantum chemical descriptors of the studied inhibitors at B3LYP/6-31G in gaseous (G) and aqueous (A) phases.

Parameter	**Gaseous Phase(G)**		**Aqueous Phase(A)**	
	P3	**P4**	**P3**	**P4**
Total Energy TE (eV)	-20368.1	-21863.3	-24880.1	-21864.1
E_{HOMO} (eV)	-14.9032	-8.5067	-8.9265	-8.9575
E_{LUMO} (eV)	-3.1430	-1.6478	-1.5371	-1.5425
Gap ΔE (eV)	11.7602	6.8588	7.3894	7.4147
Dipole moment μ (Debye)	4.8486	5.1599	8.2927	7.3082
Ionisation potential I (eV)	14.9032	8.5067	8.9265	8.9575
Electron affinity A	3.1430	1.6478	1.5371	1.5425
Electronegativity χ	9.0231	5.0772	5.1318	5.2499
Hardness η	5.8801	3.4294	3.6947	3.7074
Electrophilicity index ω	6.9231	3.7584	3.7042	3.7171
Softness σ	0.1701	0.2916	0.2707	0.2697
Fractions of electron transferred ΔN	0.1720	0.2803	0.2393	0.2360

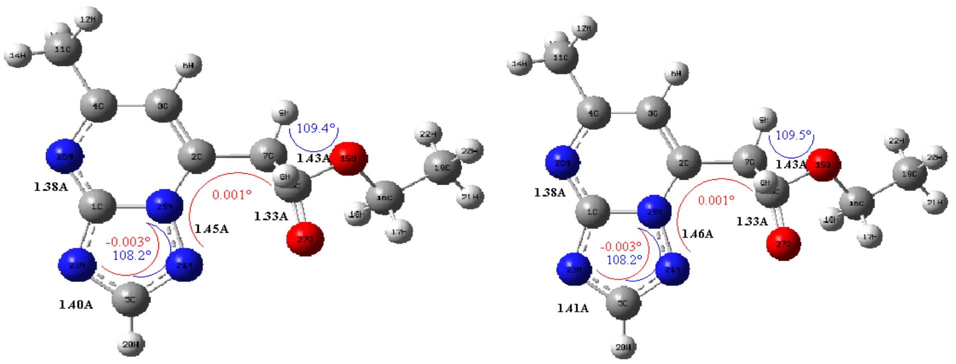

(**P3**) Gaseous phase (**P3**) Aqueous phase

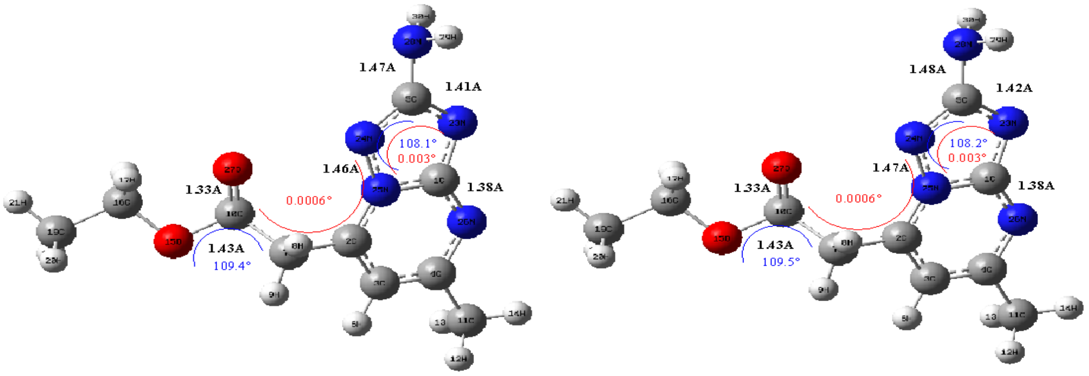

(**P4**) Gaseous phase (**P4**) Aqueous phase

Figure 8. Optimized molecular structures and selected dihedral angles (red), angles (blue) and bond lengths (black) of the studied inhibitors(P3 and P4)calculated in gaseous and aqueous phases using the DFT at the B3LYP/6-31G level

Table 6. The HOMO and the LUMO electrons density distributions of **P3** and **P4** in gaseous and aqueous phases computed at B3LYP/6-31G level for neutral forms.

Inhibitor	Type of MO	Gaseous Phase	Aqueous Phase
P3	HOMO	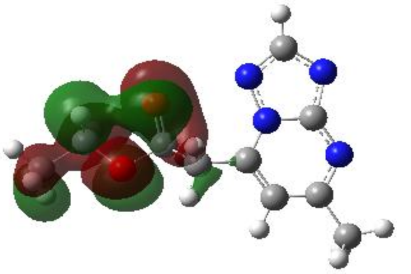	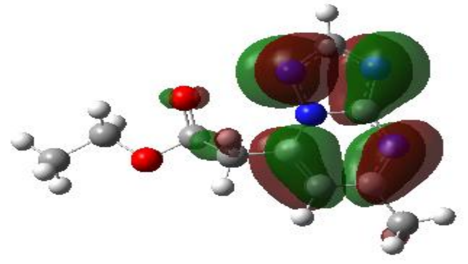
	LUMO	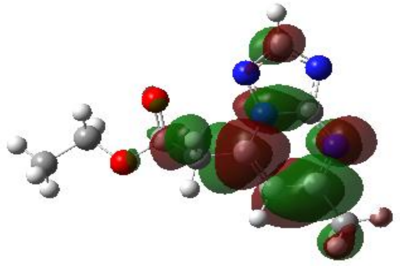	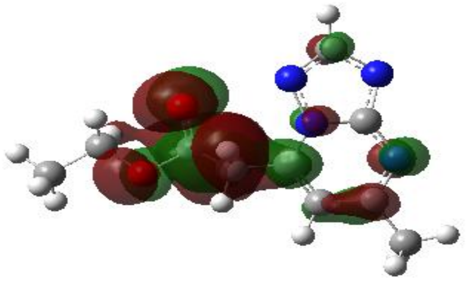
P4	HOMO	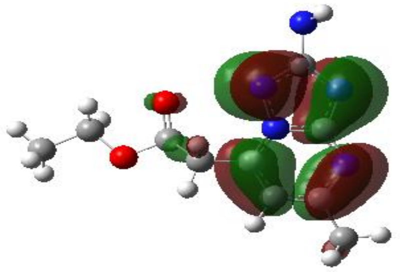	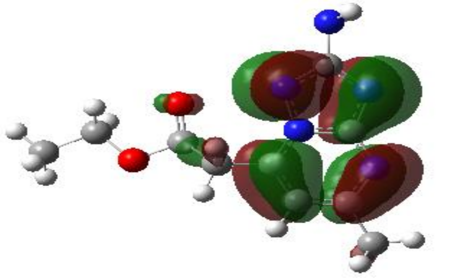
	LUMO	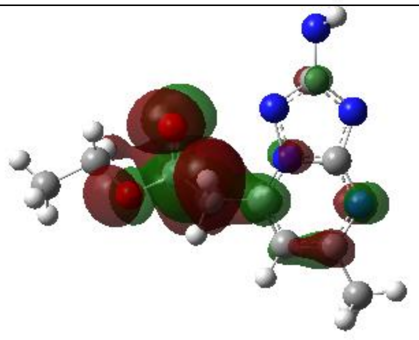	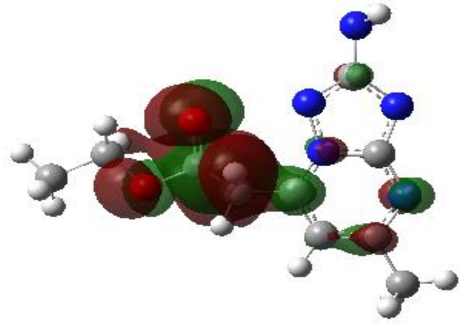

Conclusion

1,2,4-triazolo[1,5-a]pyrimidine derivatives (P3 and P4)show good inhibitive properties for the corrosion of mild steel in 1M HCl, with P4 having higher performance than P3.Comparing the methods used in this study, mass loss, electrochemical impedance spectroscopy and potentiodynamic polarization; it is clearly noticed that thy are in good agreement. EIS measurements also show that the addition of inhibitors increases the charge transfer resistance and indicate that the inhibitive performance depends on molecules adsorption on the metal surface. The polarization measurements indicate that the inhibitors P3 and P4 are act as cathodic type inhibitors. The adsorption model of compounds obeys the Langmuir isotherm at 308 K. Quantum chemical calculation by DFT method were performed to identify the reactivity of tested molecules towards corrosion inhibition, and the results are in good agreement with the experimental investigations. Both experimental and quantum chemical results showed that the inhibition efficiency of the inhibitor P4 is more than for the inhibitor P3.

References

1. Quraishi M.A &SardarR., *Corrosion.* 58 (2010) 748.
2. Abd El-Maksoud S.A&Fouda A.S., *Mater. Chem. Phys.*93 (2005)84.
3. Migahed M.A &Nassar I.F., *Electrochim. Acta.* 53 (2008) 2877.
4. Sastri V.S. &Perumareddi J.R., *Corros. Sci.* 53 (1997) 617.
5. Ahamad I., Prasad R &QuraishiM., *Corros. Sci.* 52 (2010)3033.
6. Masoud M., Awad M., Shaker M& El-TahawyM., *Corros. Sci.* 52 (2010) 2387.
7. Elmsellem H., Elyoussfi A., Steli H., Sebbar N. K., Essassi E. M., Dahmani M., El Ouadi Y., Aouniti A., El Mahi B., Hammouti B., *Der Pharma Chemica*. 8(1) (2016) 248.
8. Hasanov R., Bilge S., Bilgic S., *Corros. Sci.*52 (2010) 984.
9. Eddy N., *Mol. Simulat.*36 (2010) 354.
10. Wang H., WangX., Wang H., *J. Mol. Model.*13 (2007)147.
11. Elmsellem H., Aouniti A., Toubi Y., Steli H., Elazzouzi M., Radi S., Elmahi B., El Ouadi Y., Chetouani A., Hammouti B., *Der Pharma Chemica*. 7(7)(2015)353-364.
12. UmorenS &Ekanem U., *Chem. Eng. Comm.*197(2010)1339.
13. Elmsellem H., Harit T., AounitiA., Malek F., Riahi A., Chetouani A., Hammouti B., *Protection of Metals and Physical Chemistry of Surfaces.* 51(5) (2015) 873.
14. El-Gaby M. S. A. E.-A., Abdel-Hamide S. G., GhorabM. M. & El-Sayed S. M., *Acta Pharm*. 49 (1999) 149–158.
15. Nasr M. N &Gineinah M. M., *Arch. Pharm*. 335 (2002) 289–295.
16. Baraldi P. G., Pavani M. G., Nunez M., Brigidi P., Vitali B., GambariR &Romagnoli R., *Bioorg. Med. Chem*. 10 (2002) 449–456.
17. Sondhi S. M., Johar M., Rajvanshi S., Dastidar S. G., Shukla R., Raghubir R.,Lown J. W.,*Australian J. Chem*. 54 (2001) 69–74.
18. Chowdhury A. Z. M. S., MatinM. M &Chittagong M. N., *Univ. Stud. Part II: Sci.* 21 (1997) 79–83.
19. Mangalagiu G., Ungureanu M., Grosu G., MangalagiuI &Petrovanu M., *Ann. Pharm. Fr*. 59(2001)139–140.
20. Shishoo C. J., Shirsath V. S., Rathod I. S., PatilM. J & Bhargava S. S., *Arzneim. Forsch*. 51 (2001) 221–231.
21. Bruno O., Brullo C., Schenone S., Ranise A., Bondavalli F., Barocelli E., Tognolini M., Magnanini F., Bollabeni V., *Farmaco*.57 (2002) 753– 758.
22. Fischer G., *Heterocycl. Chem.* 57(1993) 81.
23. Barluenga J., Valdes C., Beltran G., Escribano M., Aznar F.,*AngewChemInt Ed.* 45 (2006) 6893.
24.LipshutzB. H., Taft B. R.,*AngewChemInt Ed*. 45 (2006) 8235.
25. YanZ. Y., Zhao Y. B., Fan M. J., Liu W.-M., Liang Y. M.,*Tetrahedron*.61(2005)9331.
26. Rogue D., Neill J. L.,Antoon J. W., Stevens E. P.,*Synthesis*. (2005)2497.
27. Barral K.,Moorhouse A. D., Moses J. E.,*Org Lett*.9(2007) 1809.
28. Zhang N., Semiramis A., Thai N., *J. Med. Chem*. 50 (2007) 319.
29. Havlicek L.,Fuksova K.,Krystof V., *Bioorg. Med. Chem*. 13 (2005) 5399.
30. Zhao X., Zhao Y., Guo S., Song H., Wang D., Gong P., *Molecules.* 12 (2007)1136.
31. Iwona L., Marzena F., Tadeusz M., Tadeusz S., *J. Julia, Dalton Trans*. 42 (2013) 6219.
32. Marwaha A., White J., El Mazouni F., Creason S., Kokkonda S., Buckner F., Rathod P., *J. Med. Chem*. 55 (2012) 7425.
33. Yin L.,Shuai Z., Zhi-Jun L., Hai-Liang Z., *Euro. J. Med. Chem*. 64 (2013) 54.
34. Ashraf H., *Abd El-Wahab Pharmaceuticals.* 5 (2012) 745.
35. Abdel-Aziem A., Sayed El-Gendy M., Abdelhamid A., *Euro. J. Chem*. 3 (2012) 455.
36. Khera M., Cliffe I., Mathur T., Prakash O., *Bioorg. Med. Chem. Lett*. 21 (2011) 2887.
37. Ashour H., Shaaban O., Rizk O., El-Ashmawy I., *Euro. J. Med. Chem*. 62 (2013) 341.
38. Fraley M., Hoffman W., Rubino R., *Bioorg. Med. Chem. Lett*. 12 (2002) 2767.
39. Chen Q., Zhu X., Liu Z., *Euro. J. Med. Chem*. 43 (2008) 595.

40. Uryu S., Tokuhiro S., Murasugi T., *Brain Research*. 946 (2002) 298.
41. Fettouhi M., Boukhari A., El Otmani B. &Essassi, E. M.,Acta Cryst. C52 (1996)1031–1032.
42. Gueddar H., Bouhfid R., Guessous A. R., EssassiE. M & WengNg S. ; *Acta Cryst*. E68 (2012) o239.
43. Pearson R.G., *Inorg. Chem*. 27 (1988) 734-740.
44. Sastri V.S., Perumareddi J.R., *Corrosion*. 53 (1997) 617-622.
45. Elmsellem H., Nacer H., Halaimia F., Aouniti A., Lakehal I., Chetouani A., Al-Deyab S. S., Warad I., Touzani R., Hammouti B, *Int. J. Electrochem. Sci*. 9(2014)5328.
46. Elmsellem H., Basbas N., Chetouani A., Aouniti A., Radi S., Messali M., Hammouti B., Portugaliae. *Electrochimica. Acta*. 2(2014)77.
47. Udhayakala P., Rajendiran T. V., Gunasekaran S., *Chem. J.Biol. Phys. SCI.A*. 2(3) (2012)1151-1165.
48. Benabdellah M., Aouniti A., Dafali A., Hammouti B., Benkaddour M., Yahyi A., Ettouhami A., *Appl. Surf. Sci*. 252 (2006) 8341–8347.
49. Quraishi M.A., Sharma H.K., *Chem. Phys*. 78 (2002) 18.
50. Quraishi M.A., SardarR., *Mater. Chem. Phys*. 78 (2002) 425.
51. Wang X., Yang H., Wang F., *Corros. Sci*., 52 (2010)1268.
52. Ebenso E.E., Obot I.B., Murulana L.C.,*Int. J. Electrochem. Sci*. 5(2010) 1574.
53. Migahed M.A., Mater. Chem. Phys. 93(2005) 48.
54. Wang X., Yang H., Wang F., *Corros. Sci*. 53 (2011)113.
55.Cano E., Polo J.L., La IglesiaA., BastidasJ.M.,*Adsorption*. 10 (2004) 219-225.
56. BentissF., Lebrini M., Lagrenée M., *Corros. Sci*.47 (2005) 2915.
57. Li X., Deng S., Fu H., *Corros. Sci*. 53 (2011) 302.
58. Ozcan M., SolmazR.Kardas G., Dehri I., *Colloid Surf. A*. 57 (2008)325.
59. Lebrini M., Bentiss F., Vezin H., Lagrene M., *Corros. Sci*. 8 (2006) 1279–1291.
60. Bentiss F., Traisnel M., Vezin H., Hildebrand H.F., Lagren M., *Corros. Sci*. 46 (2004) 278–279.
61. Elmsellem H., Aouniti A., Khoutoul M., Chetouani A., Hammouti B., Benchat N., Touzani R. and Elazzouzi M., *J. Chem. Pharm. Res*. 6(2014)1216.
62. Mulder W.H., Sluyters J.H., *Electrochim. Acta*. 33 (1988) 303– 310.
63. Elmsellem H., Youssouf M. H., Aouniti A., Ben Hadda T., Chetouani A., Hammouti B., *Russian, Journal of Applied Chemistry*. 87(6) (2014)744.
64. Lagrene M., B. Mernari, N. Chaibi, M. Traisnel, H. Vezin, F. Bentiss, Corros. Sci. 43 (2001) 951–962.
65. Ashassi-Sorkhabi H., Shaabani B., Seifzadeh D., *Electrochim. Acta*.50 (2005) 3446–3452.
66. F. Bentiss, M. Lagrenee, M. Traisnel, J.C. Hornez, Corros. Sci. 41 (1999) 789–803.
67. Behpour M., Ghoreishi S.M., Soltani N., Salavati-Niasari M., *Corros. Sci*. 51 (2009) 1073–1082.
68. Doner A., Solmaz R., Ozcan M., Kardas G., *Corros. Sci*. 53 (2011) 2902–2913.
69. Lebrini M., Lagrenée M., Vezin H., Traisnel M., Bentiss F., *Corros. Sci*. 49 (2007) 2254–2269.
70. Govindarajan M., Karabacak M., *SpectrochimActa Part A Mol BiomolSpectrosc*. 85(2012)251–260.
71. Khaled K.F., Abdelshafi N.S., El-Maghraby A., Al-Mobarak N., *J. Mater. Environ. Sci*. 2(2011)166.
72. Ramji K., Cairns D.R., Rajeswari S., *Appl. Surf. Sci*. 254(2008)4483–4493.
73. Elyoussfi A., Elmsellem H., Dafali A., Cherrak K., Sebbar N. K., Zarrouk A., Essassi E. M., Aouniti A., El Mahi B., Hammouti B., *Der Pharma Chemica*. 7(10)(2015)284-291.
74. Lukovits I., Kalman E., Zucchi F., *Corrosion*, 57(2001)3-7.
75. Elmsellem H., Karrouchi K., Aouniti A., Hammouti B., Radi S., Taoufik J., Ansar M., Dahmani M., Steli H., El Mahi B., *Der Pharma Chemica*, 7(10) (2015)237-245.
76. Elmsellem H., Elyoussfi A., Sebbar N. K., Dafali A., Cherrak K., Steli H., Essassi E. M., Aouniti A. and Hammouti B., *Maghr. J. Pure & Appl. Sci*. 1 (2015)1-10.

(2017) ; http://www.jmaterenvironsci.com/